Advances in Concrete Construction, *Vol. 15, No. 4 (2023) 251-267*
https://doi.org/10.12989/acc.2023.15.4.251

Assessment of the characteristics of ferro-geopolymer composite box beams under flexure

Dharmar Sakkarai*[1] and Nagan Soundarapandian [2a]

[1] *Department of Civil Engineering, Ramco Institute of Technology, Rajapalayam, Tamilnadu, India*
[2] *Department of Civil Engineering, Thiagarajar College of Engineering, Madurai, Tamilnadu, India*

(*Received September 16, 2022, Revised February 4, 2023, Accepted March 31, 2023*)

Abstract. In this paper, an experimental investigation is carried out to assess the inherent self-compacting properties of geopolymer mortar and its impact on flexural strength of thin-walled ferro-geopolymer box beam. The inherent self-compacting properties of the optimal mix of normal geopolymer mortar was studied and compared with self-compacting cement mortar. To assess the flexural strength of box beams, a total of 3 box beams of size 1500 mm × 200 mm × 150 mm consisting of one ferro-cement box beam having a wall thickness of 40 mm utilizing self-compacting cement mortar and two ferro-geopolymer box beams with geopolymer mortar by varying the wall thickness between 40 mm and 50 mm were moulded. The ferro-cement box beam was cured in water and ferro-geopolymer box beams were cured in heat chamber at 75°C - 80°C for 24 hours. After curing, the specimens are subjected to flexural testing by applying load at one-third points. The result shows that the ultimate load carrying capacity of ferro-geopolymer and ferro-cement box beams are almost equal. In addition, the stiffness of the ferro-geoploymer box beam is reduced by 18.50% when compared to ferro-cement box beam. Simultaneously, the ductility index and energy absorption capacity are increased by 88.24% and 30.15%, respectively. It is also observed that the load carrying capacity and stiffness of ferro-geopolymer box beams decreases when the wall thickness is increased. At the same time, the ductility and energy absorption capacity increased by 17.50% and 8.25%, respectively. Moreover, all of the examined beams displayed a shear failure pattern.

Keywords: box beam; ferro-cement; ferro-geopolymer; flexural behavior; self-compacting mortar

1. Introduction

m Human activities that release carbon dioxide into the atmosphere, like as the burning of fossil fuels, the production of cement, and deforestation, must end entirely if we are to stop global warming. The longer it takes, the hotter the world will become. Given the slow decarbonization pace, panic over the climate problem is understandable (Pierrehumbert 2019). Technological, institutional, and socioeconomic actions all contribute to environmental degradation. As the natural resources of Earth are exhausted, degradation takes place. Water, air, and soil are some of these resources that are impacted. The degradation affects wildlife, plants, animals, and microorganisms as well as ourselves. Numerous factors influence the environment, including urbanization, population growth, intensified agriculture, increased energy consumption, increased transportation, high levels of secondary pollutants and exhaust gases, a large number of industries, chemical effluents, and unplanned land use policies. Water pollution and scarcity, air pollution, solid and hazardous waste, soil degradation, deforestation, loss of bio diversity, and atmospheric changes are only a few of the significant environmental issues that have an impact on both productivity and health. The 3R's-Reducing, Reusing, and Recycling-are a sustainable and renewable way to live ecologically.

Resource efficiency is the ratio of added product value to the value of the resources used in production or a process thereof. The resource efficiency of a process can be separated from the resource efficiency of a product when materials, parts, and components are swapped only on the basis of their cost and usefulness. The percentage of the value of stressed resources included into a service or product that is returned after it has reached the end of its useful life is known as circularity (Francesco *et al*. 2017). Concrete's durability is defined as its ability to survive abrasion, chemical attack, and weathering while maintaining the appropriate engineering properties. Different concretes require differing degrees of durability depending on the exposure environment and targeted attributes (Portland Cement Association 2019).

A simply supported reinforced concrete beam has two zones, one, above the neutral axis which is known as the compression zone and the other, below the neutral axis, known as the tension zone. Steel reinforcements are placed in the tension zone because concrete is weak in tension. Between the compression and tension zones, the concrete below the neutral axis serves as a stress transfer medium. Concrete that is located below the neutral axis experiences the least amount of stress and is known as sacrificial

*Corresponding author, Ph.D., Head,
E-mail: dharmar.msd7@gmail.com
[a] Professor, E-mail: nagan_civil@tce.edu

ISSN: 2287-5301 (Print), 2287-531X (Online)

concrete. Lightweight materials such as expanded polystyrene, PVC pipes, aerated blocks, bricks, etc. can be used in place of this sacrificial concrete. Box or hollow beam is the name given to that kind of beam with a hollow or rectangular cross section. Parthiban and Neelamegam (2017) investigated the flexural behaviour of a reinforced concrete beam with a hollow core in shear section. Rectangular FRP-tube beams with full and partial concrete fills had their structural performance tested under flexure in order to evaluate the ductility and strength-to-weight ratio of the beams experimentally, and the findings were compared with analytical analysis (Ahmed and Radhouane 2015). Ibrahim *et al*. (2018) tested the flexural properties of light-weight reinforced concrete beams using various types of core materials and mesh reinforcement.

Thin-shell concrete, commonly referred to as ferro-concrete or ferro-cement, is a system of reinforced plaster or mortar that is put over a layer of metal mesh or woven expanded-metal or metal fibres, and closely spaced thin steel rods like rebars. Pier Luigi Nervy, an Italian engineer, architect, and builder, performed the first ferro-cementing operation on buildings, ships, and aeroplane hangars in 1940. The flexibility, affordability, and durability qualities of this material are outstanding. The ACI Committee 549 (1997) describes ferro-cement as a kind of thin wall with a medium thickness that is constructed utilising a hydraulic concrete mixture along with wire mesh layers. Hexagonal, welded, woven, and three-dimensional meshes are the four basic forms of wire mesh used in the building sector. A suitable metal or other material can be used to make the mesh. The thickness ranges from 25 to 60 millimetres. For the flexural analysis and design of ferro-cement members, various investigations are accessible. However, when using unmodified cement mortar, ferro-cement elements do develop cracks under some loads that are much smaller than the ultimate load and have durability issue. The ability of a structure to withstand weathering, abrasion, chemical attack, cracking, or any other form of deterioration is referred to as durability. One of the main causes of ferro-cement degradation is corrosion of the reinforcement. Sakkarai and Soundarapandian (2021) investigated the strength behavior of flat and folded fly ash-based geopolymer ferrocement panels under flexure and impact. Aofei *et al*. (2021) performed experimental and finite element analysis on mortar beams made of chemically altered kenaf fibres to assess their effect on the flexural behaviour of mortar.

The permeability of the cement mortar has a major role in the corrosion of reinforcement. Therefore, corrosion can be minimised in ferro-cement mortar by carefully choosing the chemical and mineral additives, as well as the water to cement ratio. The pore size is subsequently decreased, leading to extremely high strength and durability levels, and the flexural moment capacity of ferrocement elements rises with the volume fraction of reinforcement. Shannag and Mourad (2012) conducted a laboratory investigation to develop high strength cementitious matrices that contain fly ash and silica fume and provide a good balance between flowability and strength for casting thin ferrocement laminates that are perfect for structural repair/retrofit.

In a report titled "Global Warming Effect on the Cement and Aggregates Industry," Davidovits (1994) presented the results of the calcination of limestone (calcium carbonate) and silico-aluminous material to produce cement (ordinary Portland cement). A direct result of producing 1 tonne of cement is the production of 0.55 tonnes of chemical CO_2. In iron metallurgy, the iron ore, Fe_2O_3, is reduced into FeO and Fe, coke is burned, and limestone is decarbonized. In the bottom of the blast furnace, above the pig iron, is the by-product known as blast furnace slag. By-products from the manufacturing of one tonne of iron include 0.6 tonnes of iron slag and 0.19 tonnes of chemical CO_2. Contrary to popular opinion, cement manufacture produces 8 times more chemical-CO_2 emissions than emissions resulting from metallurgical activities. The production of 1 tonne of cement which directly generates 0.55 tonnes of chemical-CO_2, requires the combustion of carbon-fuel to yield an additional 0.40 tonnes of carbon-dioxide. To simplify: 1 T of cement = 1 T of carbon-dioxide.

Cement production has increased significantly globally in recent years, according to data accessible with UNFCCC, and is now the third-largest source of anthropogenic carbon dioxide emissions, behind fossil fuels and land use change. In 2016, the total emissions from processes around the world were 1:45_0:20 $GtCO_2$, equivalent to about 4% of emissions from fossil fuels. Cumulative emissions from 1928 to 2016 were 39:3_2:4 GtCO2, 66% of which have occurred since 1990 (Robbie 2018).

A new all-time record of 36.8 Gt for global carbon dioxide (CO_2) emissions from industrial processes and energy combustion was reached in 2022, up 0.9% or 321 Mt. Following two years of unusual fluctuations in emissions connected to energy, there was a rise last year. The Covid-19 epidemic decreased energy demand in 2020, resulting in a greater than 5% decrease in emissions. As a result of economic stimulus measures and the widespread use of vaccines, emissions in 2021 increased above pre-pandemic levels and increased by more than 6%. While industrial process emissions declined by 102 Mt, emissions from energy combustion increased by 423 Mt. (IEA 2022). From 2015 to 2021, the direct CO_2 intensity of cement manufacturing grew by around 1.5% year. As a contrast, the Net Zero Emissions by 2050 Scenario requires 3% yearly decreases through 2030. Two crucial areas require further attention: lowering the clinker-to-cement ratio (especially by promoting blended cements) and implementing cutting-edge technology, like carbon capture and storage and clinkers produced from alternative source materials. In order to create mortar/concrete that is more environmentally friendly, it is necessary to locate a different kind of binder. The use of by-product materials like fly ash, in place of cement, is a promising alternative.

Kuhl (1908) made some innovative and helpful improvements in "slag cement and procedure of manufacturing the same,". In his further research, he produced a solid substance similar to hardened Portland cement by using an alkali source to activate a reaction with a solid precursor that contained alumina and silica.

Purdon was historically the first to make improvements to the use of alkali-activated cement in the 1940s. In his

research, Purdon created chemically activated materials by combining sodium hydroxide as an activating solution with blast furnace slag as a precursor. Throughout the previous century, alkali-activated cement was the subject of research. Later in 1957, Glukhovsky created "alkaline/soil-cement," a new kind of binder made from alumina silicate combined with industrial wastes high in alkalis. The term was given to the new substance because it resembled ground rock in form and aspect and also had cementitious properties.

Provis and Van Deventer was published (2009) a book titled "Geopolymers-Structure, Processing, Properties and Industrial Applications". They provided a brief review of the key elements of geopolymer technology, including its historical development and the terminology used to define geopolymers. Also, a scientific introduction to geopolymer technology is provided. Alkali-activated slags and other related materials are not included in the scope of this review, which is restricted to mostly low calcium materials, or "traditional" alkali-aluminosilicate geopolymers.

Palomo *et al*. (2014) are reviewed the most important theoretical explanations of the function performed by alkalis in the development of the "stony" structure of cement. It concludes with a general overview of the adaptability of this kind of materials for industrial applications and a discussion of the possibilities of building on existing legislation to meet the need for the regulation of the production of alkaline cement and concrete in the future.

Provis (2014) is reviewed the alkali-activation technology, spanning from the atomic scale and chemical reaction path modelling to macroscopic observables including the strength and durability of alkali-activated concretes.

As a result of several fires that occurred frequently in Europe, scientists were forced to create a material that could withstand such an assault. Consequently, the French scientist and engineer Prof. Joseph Davidovits (Davidovits 1979), developed a category of solid materials known as "geopolymers" that were created by the reaction of an alumina-silicate powder with an alkaline solution. These novel materials had the ability to change and polycondense like "polymers" since they are inorganic, hard and stable at high temperature and also inflammable. When Al-Si minerals are subjected to a chemical reaction under extremely alkaline circumstances, polymeric Si-O-Al-O linkages are produced.

In Palomo *et al*. (2021), a thorough review of the vast body of literature on alkali-activated binders (AABs) in construction is conducted. The authors' primary goal is to conclusively rebut claims made by those in the scientific community who undervalue or even ignore the possibility of AABs as Portland cement substitutes (PC). The review also examines the function of alkaline activators in the chemistry of AABs; it is crucial to clarify and emphasise that alkaline activators are not, by any means, limited to the two synthetic products (caustic soda and water glass) that are frequently used by researchers; other readily accessible, efficient, and sustainable products are also available. The review also discusses the adaptability of AAB production methods. The final takeaways from this review study concern the one-part AABs' low carbon footprint and the urgent need to investigate standardized formulas that would permit the commercial production of (sustainable) binders other than PC.

Davidovits (1994) produced a concrete mixture geopolymer composite material by including a pozzolanic ingredient and alumina silicate from an extremely alkaline solution. Fly ash, which is commonly obtained from coal power stations, is a great primary material for alumina silicate. It also demonstrates ceramic properties like strong fire resistance at high temperatures. Abdulla *et al*. (2011) quantitatively exhibited the operation and chemical reactivity of fly ash-based geopolymer concrete. Peng *et al*. (2020) evaluated the workability, compressive strength, flexural performance, elastic modulus, and fracture property of fly ash (FA) and metakaolin (MK) based geopolymer/ alkali-activated mortar modified with polyvinyl alcohol (PVA) fibre and nano-SiO_2.

The greatest tool for assessing the environmental impact of alkali-activated cements and concrete (AACC)s is life cycle assessment (LCA). To compare AACC with ordinary concrete, Ouellet-Plamondon and Habert (2015) suggested a new approach based on the Feret equation that highlights the intrinsic qualities of the binder that requires the concrete strength and a constant amount of paste (cement + water). The environmental benefit of alkali-activated cement is significantly diminished when environmental effects other than global warming potential (GWP) are taken into account. Bricks, partial geopolymers, and hybrid cement are the three AACC future trends. Hence, the development of geopolymer mortar (GM), an ecologically sustainable substance that can replace Portland cement, was one of the most significant advances in the field of new materials. Innovative geopolymer concrete, which completely replaces OPC, is manufactured. As a result, the use of geopolymer technology not only significantly reduces CO_2 emissions from the cement industry but also makes use of industrial waste and/or byproducts of aluminium silicate composition to produce added-value construction materials. But during the past ten years, a lot of study has been done on fly ash to assess the likelihood of using coal fly ash as an alumina-silicate source material. The majority of earlier research focused on the synthesis of geopolymers from metakaolion. Fly ash has the potential to be one of the sources of silica alumina for geopolymer binders. Numerous research studies have revealed the possible application of fly ash-based geopolymer mortar. Low-calcium fly ash provides a fundamental component for the synthesis of geopolymer, allowing the efficient utilisation of this industrial waste.

The primary focus of the research by Hardjito *et al*. (2008) was the low calcium fly ash-dependent geopolymer mortar's setting time. Tran *et al*. (2009) studied how the curing temperature of carbon-reinforced composites made of silica affected their flexural properties. An ideal curing temperature for achieving a satisfactory flexural strength was found to be between 70°C and 100°C. Temuujin *et al*. (2010) examined experimentally the formulation and characterization of geopolymer mortar made of fly ash by altering the binding substance and aggregate proportion. For fly ash geopolymer mortars activated with mixed sodium silicate and sodium hydroxide solutions, Naghizadeh and

(a) River sand

(b) Fly ash

(c) Sodium hydroxide flakes

(d) Sodium silicate solution

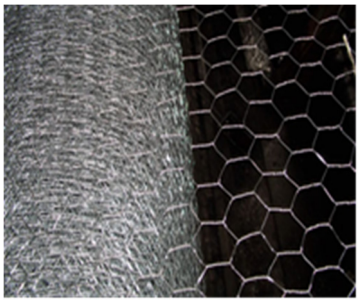

(e) Chicken wire mesh

(f) Super plasticizer

Fig. 1 Constituents of the geopolymer ferrocement

Ekolu (2019) established a new mix design methodology. The proposed technique concept can be used to produce appropriate mix design charts for various geopolymer binders. Following a thorough examination using Preferred Reporting Items for Systematic Reviews (PRISMA), Nabila *et al*. (2022) conducted a review of Geopolymer Concrete (GeoC). This study looks at the potential of GeoC as a green building material in terms of recent applications, sustainable growth, and circular economy.

Due to its high viscosity, the low workability of a fresh fly ash-based geopolymer could be a considerable disadvantage. Xie and Kayali (2016) looked at how superplasticizer affected the Class F and Class C workability of fly ash-based geopolymers. Superplasticizers based on polycarboxylates were successful for Class C fly ash, whereas those based on naphthalene were successful for Class F fly ash.

In reality, complete compaction is practically the only need for any concrete. Full compaction is difficult to guarantee in the event of large, thin, and complex structures, such as ferro-cement structures. Even with a proper mix design, poor compaction dramatically reduces concrete's final performance. In order to get the maximum strength and durability of the hardened concrete, the placement of the fresh concrete requires expert workers to ensure sufficient compaction. There are concerns concerning the strength and durability of concrete placed in such locations as it is made and deposited at building sites, where there may be risks to the workers. Utilizing self-compacting concrete or mortar is one way to get over these obstacles. A relatively new concept, self-compacting geopolymer concrete (SCGC)/mortar is regarded as the most inventive development in concrete technology. SCGC is a revolutionary type of concrete that can be produced without the need for vibration during installation because normal Portland cement has been completely eliminated from the mix. Abdulkadir *et al*. (2020) conducted an analysis of the applicability of prefabricated cage-reinforced composite beams with self-compacting and lightweight concrete under flexural loads. In order to provide a reasonable mix-design process and self-compactibility testing methodologies for self-compacting concrete, Hajime Okamura and Ouchi (2003) conducted research.

The major objective of this research is to create an eco-friendly composite material for construction that can incorporate industrial by-products and be used as a flexible building component by combining the advantages of ferrocement and geopolymer technologies. A study is also undertaken to look into how the strength of geopolymer ferrocement box beams behaves under flexure by altering the wall thickness of the box beams for optimization and improved performance.

2. Materials and methods

2.1 Materials

Fig. 1 illustrates the constituents of geopolymer ferrocement.

2.1.1 River sand

In accordance with Zone II of IS 383 (1971), 2.36 mm IS sieved river sand that was retained on a 150 micron IS sieve of 2.69 specific gravity and 2.82 fineness modulus was used as the fine aggregate.

2.1.2 Fly ash

The chemical parameters of the low calcium fly ash (Class F) which was obtained from the Tuticorin thermal

Table 1 Low-calcium fly ash chemical compositions

Properties	Configuration (% by mass)	Limits as per IS 3812 (Part 1) (2013) (% by mass)
Silicon di Oxide (SiO_2) + Aluminium Oxide (Al_2O_3) + Iron Oxide (Fe_2O_3)	90.06	70.00 (Min.)
Silicon di Oxide (SiO_2)	47.75	35.00 (Min.)
Magnesium Oxide (MgO)	0.70	5.00 (Max.)
Total Sulphur [Sulphur tri Oxide (Na_2O)]	0.48	3.00 (Max.)
Alkalis [Sodium Oxide (Na_2O)]	0.21	1.50 (Max.)
Loss on Ignition	1.73	5.00 (Max.)

Table 2 Characteristics of sodium hydroxide

Characteristics	Data
Physical characteristics	
Colour	Colourless
Specific gravity	1.47
P^H	14
Chemical characteristics	
Assay	97%
Carbonate (Na_2Co_3)	2%
Chloride (Cl)	0.02%
Sulphate (So_4)	0.01%
Lead (Pb)	0.002%
Iron (Fe)	0.005%
Potassium (K)	0.1%
Zinc (Zn)	0.02

power plant and conforms to IS 3812 -Part 1(2003) and ASTM C618-5 (2005), is listed in Table 1. The utilized fly ash has a specific gravity of 2.32 and a fineness of 390.40 m^2/kg, respectively.

2.1.3 Sodium hydroxide

According to the instructions in Perry's Chemical Engineers' Handbook (Perry 1997), the sodium hydroxide solids and water necessary to produce a sodium hydroxide solution with the required molarity were extracted. Table 2 lists sodium hydroxide's characteristics based on information from the manufacturer.

Table 3 Characteristics of sodium silicate

Characteristics	Data
Chemical equation	Na_2SiO_3
Na_2O	15.90 (%)
SiO_2	31.40 (%)
H_2O	52.70 (%)
Form	Liquid (Gel)
Tint	Light yellow
Boiling point	102°C (for 40% aqueous solution)
Molecular weight	184.04 (g/mol.)
Specific gravity	1.60

2.1.4 Sodium silicate

The chemical compound sodium meta silicate, Na_2SiO_3, is sometimes referred to as sodium silicate, water glass, and liquid glass. It comes in solid and liquid forms and is used in the manufacture of cement, passive fire prevention, refraction, textile and lumber processing, and in automobiles. Table 3 lists the characteristics of sodium silicate based on the information from the manufacturer.

2.1.5 Wire mesh

As the primary mesh reinforcement, steel wire meshes were utilized. The size, ductility, manufacture, and treatment of the mesh used in the beam have an impact on the final ferro-cement component's properties. This type of mesh is accessible, reasonably priced, and simple to use. Cold drawn wire, typically twisted into hexagonal forms, makes up this mesh. A hexagonal mesh with longitudinal wires may have special patterns. Fig. 1(e) illustrates the galvanized wire mesh that was used for this project. With

Table 4 Parameters of super plasticizer

Parameters	Data	Limits as per IS:9103-1999
Physical condition & Color	Liquid & Light brown liquid	Liquid & Light brown
Active ingredient's chemical name	Sulphonated Naphthalene Polymers	Sulphonated Naphthalene Polymers
Relative density (at 25ºC)	1.081	1.09 + 0.01(Max.)
pH	7.04	6.00 (Min.)
Content of chloride ions (%)	Nil	0.20 (Max.)
Content of dry materials (%)	34.59	34 + 5 (Max.)

Fig. 2 Reinforcement detailling of box beam

Table 5 Quality of water for mixing and curing

Properties	Test results	Limits as per IS 3025 (1987) & IS 1489 (Part 1) (2005)
P^H	7.5	≥ 6
Chloride	266 mg/l	< 500 mg/l
Sulphate	345 mg/l	< 400 mg/l
Suspended material	620 mg/l	< 2000 mg/l
Total Hardness	400 mg/l	300 – 600 mg/l

a width of 0.72 mm and a gauge of roughly 20, the wire spacing is 12.50 mm c/c. Prior to being inserted into the panel mould, the steel mesh wire was bound into the ideal position as depicted in Fig. 2(c). Chicken wire has a yield strength of 310 N/mm^2.

2.1.6 Super plasticizer

A water reduction admixture, such as Fosroc Conplast SP430 and a chloride-free super plasticizing admixture based on certain sulphonated naphthalene polymers, according to IS 9103 (1999) and ASTM C494 (1999), Type 'F' and Type 'A', are employed to provide the required workability. Based on the data from the manufacturer, Table 4 summarizes the characteristics of super plasticizer.

2.1.7 Beam reinforcement

The beam is reinforced by two 8mm-diameter hanger bars at the top and four primary bars of 12 mm diameter at the bottom manufactured of HYSD Fe 415 steel that complies with IS 1786 (2008). All four sides surround the chicken wire mesh. The reinforcing details are shown in Fig. 2.

2.1.8 Water

It was necessary to mix and cure the ferro-cement beam with potable water that complied with IS 3025 (Part 1) (1987) and IS 1489 (Part 1) (2005), as well as to create the activator solution for the ferro-geopolymer box beams and control specimens. The Table 5 displays the water quality that was used.

2.1.9 Expanded polystyrene

The beam with a rectangular hollow cross section was made using expanded polystyrene, as shown in Fig. 2.

2.1.10 Alkaline activator solution

Twenty-four hours before the application, an activator solution was created using sodium hydroxide and sodium silicate solutions.

2.1.11 Geopolymer mortar

To make geopolymer mortar, the pozzolanic component was synthesised using a mixture of activator solution. The components of the freshly formed mortar are liquid alkaline activator, fine aggregate, and fly ash. Prior to merging, each quantity of each substance was weighed using the mix design. 24 hours in advance, alkaline activator solutions were made, and were allowed to cool to ambient temperature. It was then combined and cast. The weighted components were combined using a drum mixer. After three minutes of dry mixing, alkaline liquid was added to the mixture. After being diluted in additional water, a superplasticizer was additionally added to the mixture. It took 4 minutes to complete the wet mixing to create geopolymer mortar specimens. It was then poured into the moulds.

2.1.12 Mix proportions of mortar

The ranges of mix proportions for structural ferrocement applications must be sand cement ratio by weight, 1 to 3, and water cement ratio by weight, 0.30 to 0.45, according to Bangladesh National Building Code – Part 6 (2012) and the Maharastra Government WRD Handbook (2018). Additionally, the mortar's 28-day compressive strength must be at least 35 N/mm^2. Fresh mortar slump is typically limited to 50 mm. Trial mixes are made in accordance with the mix proportions provided in Tables 6 and 7 in order to establish the ideal mix percentage for fabricating box beams while keeping in mind the aforementioned recommendations and EFNARC norms (2002) for self compacting concrete.

2.2 Geometry and cross section of the box beams

Fig. 3 shows the box beam's geometry as it was used in the experimental investigation. The wall thickness of the ferro-geopolymer box beams (GFBB-T40 and GFBB-T50) varies and is shown in Table 8 along with a description of the box beams.

Table 6 Mix proportions of cement mortars

Mix ID	Water / Cement ratio	Binder		Super plasticizer (% of binder)	Fine aggregate (Sand)
		Cement	Fly ash		
CM* 1:1	0.30 0.35 0.45	1	-	1	1
CM 1:2	0.30 0.35 0.45	1	-	1	2
CM 1:3	0.30 0.35 0.45	1	-	1	3
SCCM 1:1	0.30 0.35 0.45	0.60	0.40	1	1

*CM: Cement Mortar; SCCM: Self-Compacting Cement Mortar

Table 7 Mix proportions of geopolymer mortars

Mix ID	Water / Cement ratio	Fly ash (Binder)	Super plasticizer (% of Fly ash)	Molarity of NaOH (M)	Na_2Sio_3 / NaOH	Fine aggregate (Sand)
GM* 1:1	0.30 0.35 0.45	1	1	10	1	1
GM 1:2	0.30 0.35 0.45	1	1	10	1	2
GM 1:3	0.30 0.35 0.45	1	1	10	1	3

*GM: Geopolymer Mortar

Table 8 Description of box beams

Description of box beams	Beam ID
40 mm wall thickness ferro-cement box beam	FBB* – T40
40 mm wall thickness ferro-geopolymer box beam	GFBB –T40
50 mm wall thickness ferro-geopolymer box beam	GFBB –T50

*FBB: Ferro-Cement Box Beam;
GFBB: Ferro-Geopolymer Box Beam

2.3 Casting and curing of specimens

Steel moulds (Fig. 4) that had been properly lubricated were used to cast the specimens. The prepared mortar was applied to the reinforcement and then compacted firmly. Traditional cement and geopolymer mortar were put through a consistency test using flow table testing in accordance with BS EN 1015-3 (1999). Segregation resistance, passage ability, and filling ability are characteristics of SCC, according to EFNARC recommend-dations. To assess the qualities of self-compacting mortar, the following tests were used: V-funnel test (filling ability), J-ring test, L-box test, and V-funnel test at T_5 minutes

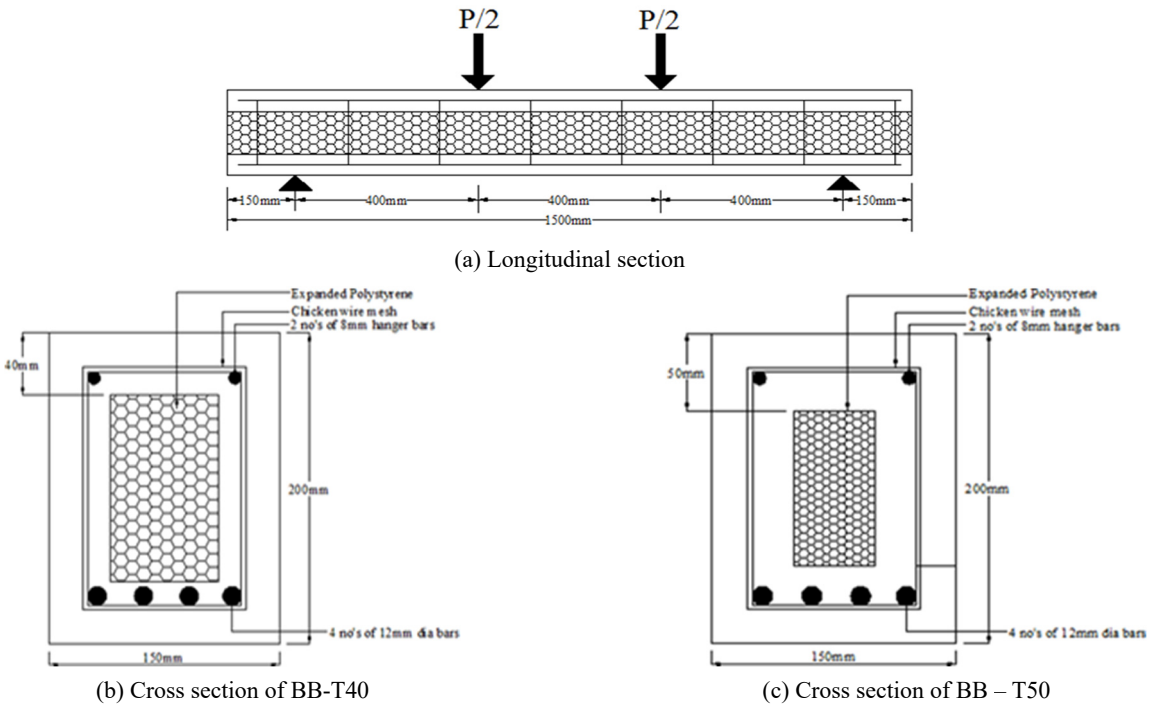

(a) Longitudinal section

(b) Cross section of BB-T40

(c) Cross section of BB – T50

Fig. 3 Geometry and cross section of box beams

(a) Reinforcement cage with EPS insert

(b) Casting of box beam

(c) Specimen under water curing

(c) Cross section of BB – T50

Fig. 4 Casting and curing of box beams

Fig. 5 Box beams after curing

(segregation resistance). Mortar cubes of size 70.6 mm × 70.6 mm × 70.6 mm were also formed to measure the usual stiffness of the geopolymer and cement mixture. After 24 hours, the specimens were demolded and heated in a specially constructed heat curing chamber for 24 hours at 75°C to 80°C for geopolymer-based specimens and water curing for cement-based specimens (Fig. 4(c) and (d)). Fig. 5 displays box beams that have been tested after curing.

2.4 Test methods

2.4.1 Tests on control specimens

According to the same standards as the OPC mortar, the geopolymer mortar cubes were cast and subjected to testing.

(a) Compressive strength test on mortar cubes

(b) Split tensile test on mortar cylinders

Fig. 6 Tests on control specimens

(a) J-ring test

(b) V-funnel test

(c) L-box test

(d) Mortar preparation

Fig. 7 Tests on fresh self-compacting mortar

The compressive strength of mortar cubes with dimensions of 70.6 mm × 70.6 mm × 70.6 mm was initially evaluated in accordance with IS: 4031 (Part 6) (1988). Splitting tensile strength tests were carried out on cylinders measuring 75 mm × 150 mm in accordance with IS 5816 (1999). Tests were performed on geopolymer mortar specimens with a cross section of 100 mm × 100 mm × 500 mm without mesh reinforcement in a UTM with a 1000 kN capacity (Fig. 6(b)). Mortar cubes and cylinders were tested for compressive strength and splitting tensile strength in a compressive testing equipment with a 1000 kN capacity (Fig. 6(a)).

Tests on fresh mortars

In addition to the slump test, BS: EN 1015-3 flow table testing was used to evaluate the consistency of regular

cement and geopolymer mortars. According to EFNARC recommendations, the V-funnel test (filling ability), J-ring test & L-box test (passing ability), and V-funnel test at T_5 minutes (segregation resistance) were performed to evaluate the properties of self-compacting mortar (SCM) (Figs. 7(a)-(c)). A drum mixer was used to prepare the mortar (Fig. 7(d)).

Impact test using drop-weight

The ability to absorb energy, or "toughness," becomes extremely important when mesh-reinforced composites are put under static, dynamic, and fatigue loads. The drop-weight impact test is a method for determining how well composites consisting of cement and concrete withstand impacts. According to ASTM D 2794-93 (2010), the impact test was conducted using a 4.5 kg hammer that was allowed to freely fall through a guide at the centre of cement and geopolymer mortar discs measuring 150 mm in diameter from a constant height of 460 mm. The specimens were placed on a stable platform in their correct places. After the mass was repeatedly dropped, the number of drops necessary to eventually cause the first crack was recorded for each panel. The process was continued up until a visible crack appeared on the upper surface of the specimen. The same number of blows were recorded at this time. The impact test setup is shown in Fig. 8.

Fig. 8 Drop-weight impact test on mortar disc

2.4.2 Non-destructive tests (NDT) on ferro-cement and ferro-geopolymer box beams

The compressive strength of geopolymer mortar cubes that represented the appropriate combinations was evaluated in accordance with IS 4031 (Part 6) (1988) in a compressive testing machine with a 1000 kN capacity (Fig. 6(a)).

Test of ultrasonic pulse velocity (UPV)

To verify the quality and uniformity of the box beams (Fig. 9), an ultrasonic pulse velocity test was performed. In order to conduct this test, an ultrasonic pulse was sent through the beams, and the time it took for the pulse to pass through was recorded. Lower velocities could be an indication of cracks or cavities in the beam, whereas higher velocities show strong material quality and continuity.

Rebound hammer test

These objectives guided the rebound hammer test that was performed (Fig. 10): (1) The compressive strength of the geopolymer mortar may be determined by relating the rebound index to the compressive strength. (2) To check for uniformity in the geopolymer matrices within the beams. (3) To assess the relative merits of various beams.

Fig. 10 Rebound hammer test on box beam

Fig. 9 Ultrasonic pulse velocity test on box beams

(a) Loading frame with hydraulic jack, load cell and LVDT

(b) Data logger with PC interface & printer

Fig. 11 Flexure test setup on box beam

Table 9 Workability properties of self-compacting cement and geopolymer mortars

Tests	SCCM-1:1			GM-1:1			Acceptance criteria as per guidelines		
Activator/binder ratio	0.30	**0.35**	0.45	0.30	0.35	**0.45**	Unit	Min.	Max.
J-ring test	3.00	**8.50**	11.50	5.00	8.50	**9.50**	Mm	0	10
V-funnel test	14.00	**11.00**	4.00	16.00	14.00	**6.00**	Sec	6	12
V-funnel at T_5 minutes test	16.00	**13.00**	6.00	18.00	13.00	**8.00**	Sec	0	+3
L-box test	1.20	**0.93**	0.50	1.40	1.10	**0.90**	h1/h2	0.80	1

2.4.3 Flexure test on ferro-cement and ferro-geopolymer box beams

Box beams made of ferro-cement and ferro-geopolymer are employed in the study. One ferro-cement box beam and two ferro-geopolymer box beams, each measuring 1500 mm × 150 mm × 200 mm, were cast using cement and geopolymer mortar and then flexure tests were conducted on them. On a loading frame with a 50-ton capacity, a hydraulic power pack system, hydraulic jack and all the beams are put through their paces. Through a load cell with a 20-ton capacity, the loads are applied in small increments of around 2 kN (Fig. 11(a)). The deflections at the bottom centre of the beam were simultaneously recorded for each increment of load up until failure using a 0-50 mm LVDT. The load cell is connected to the LVDT via a PC interface and the Universal Data Acquisition System (Fig. 11(b)). The cracking, ultimate, and failure loads, as well as the associated deflections, were also captured by the data acquisition system. The cracking pattern was closely monitored throughout the loading process. The results of the beams' flexure tests, including the cracking load energy absorption, stiffness, ductility, and ultimate load are summarised in Table 9. The load-deflection curves for each beam are also plotted.

3. Test results and discussions

3.1 Test results of fresh and hardened mortars

3.1.1 Self-compacting characteristics of cement and geopolymer mortar

In accordance with EFNARC specifications and guidelines, the workability of self-compacting mortar is evaluated using the J-ring test (passing ability), V-funnel test (filling ability), V-funnel at T_5 minutes test (secregation resistance), and L-Box test (passing ability). The results are shown in Table 9.

Table 10 Compressive strength of cement mortar and geopolymer mortar

Mortar ID	Compressive strength (N/mm^2)			Curing adopted
Activator/binder ratio	0.30	0.35	0.45	
CM 1:1	42.00	**45.63**	39.48	Water curing for 28 days
CM 1:2	40.90	44.20	37.80	
CM 1:3	38.20	42.90	33.70	
SCCM 1:1	44.00	**47.00**	41.00	
GM 1:1	40.00	42.50	**47.40**	Heat curing for 24 hours @ 75°C – 80°C.
GM 1:2	39.80	41.40	42.80	
GM 1:3	37.80	38.60	39.50	

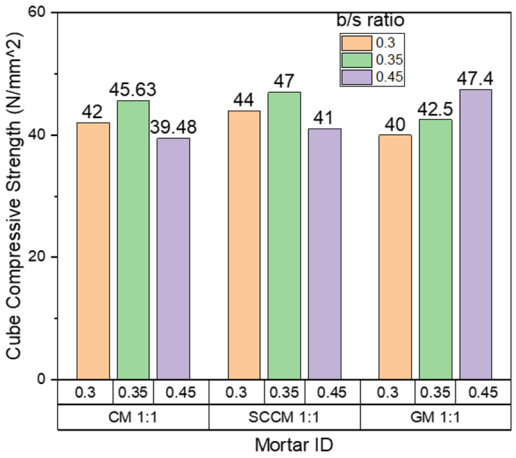

Fig. 12 Cube compressive strength of cement and geopolymer mortars

According to the test results, the self-compacting cement mortar mix SCCM-1:1 with water/binder ratio 0.35 and the standard geopolymer mortar mix GM-1:1 with activator solution/binder ratio 0.45 both met the requirements for self-compacting mortars' workability properties as set forth by EFNARC. **As a result, it has been established that geopolymer mortar has inherent self-compacting capabilities.**

3.1.2 Compressive strength of cement mortar and geopolymer mortar

The compressive strength of cement and fly ash-based geopolymer mortar specimens is shown in Table 10 and Fig. 12.

According to the test results, the conventional geopolymer mortar mix GM-1:1 with solution/binder ratio of 0.45 and the cement mortar mix SCCM-1:1 with water/binder ratio of 0.35 both produced higher compressive strengths. Additionally, the compressive strength of geopolymer mortar is around 3.88% higher than that of regular cement mortar. This rise might be explained by the geopolymer's capacity to fill pores, which finally leads to a densely packed microstructure. When comparing the results for different water-cement ratios in the cement mortar mix, there is a loss in strength for a water-cement ratio of 0.45. As determined, the typical cement mortar mixture for ferro-cement beams consists of a 1:1 binder ratio and a 0.35 water to cement ratio. It is decided to use GM 1:1 with a solution-binder ratio of 0.45 and a sodium hyroxide solution concentration of 10M for ferro-geopolymer beams.

3.1.3 Impact resistance, impact strength, and impact energy absorption of mortars

According to ASTM D2794-93, a 4.5 kg free falling hammer was used in the impact test via a guide in the middle of the specimen from a fixed height of 460 mm. The overall energy absorbed by the specimen when it is struck by a hard impactor depends on the local energy absorbed in the contact zone as well as by the impactor. The following formula can be used to determine the energy absorption

$$E = N(w\ h) \tag{1}$$

where, E = Energy in joules; w = weight in Newton; h = drop height in meter; N = blows in numbers.

The ratio of energy received at specimen failure to energy absorbed at the first crack's initiation is known as the "Residual Impact Strength Ratio". The impact resistance, impact strength, and impact energy absorption of mortars are displayed in Table 11 and Fig. 13.

Mortar disc's impact resistance, energy absorption, and residual impact strength ratio are calculated both at the initial and the ultimate cracks. The impact resistance of the geopolymer mortar increased by 16.80% when compared to cement mortar, but the impact strength decreased by 14.30%, and the energy absorbed at failure due to impact remained constant. Punching shear is found to be the impact-related failure pattern of the tested specimens.

3.2 Test results of box beams

3.2.1 Rebound hammer test results

This method, which complies with IS 13311 (Part 2) (2004), uses the suitable co-relations between rebound index and compressive strength to calculate the compressive strength of concrete/mortar. It is also used to evaluate the homogeneity of concrete. The test was run on the grid

Table 11 Impact resistance, impact strength, and impact energy absorption of mortars

Mortar ID / Activator-binder ratio	Hammer drop (Number of blows)		Impact resistance (%)	Impact strength ratio	Impact energy apsorption at ultimate (Joule)
	At the initiation of first crack	At ultimate			
SCCM-1:1/0.45	5	7	71.43	1.40	46.82
GM-1:1/0.45	6	7	88.24	1.20	46.82

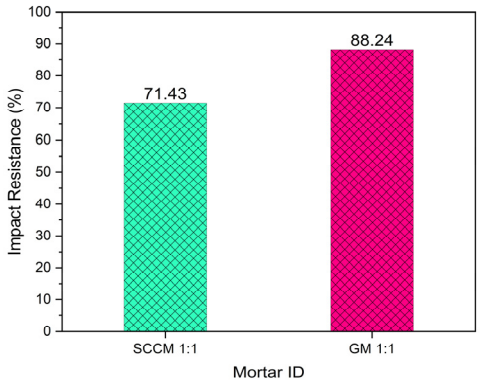

(a) Impact resistance

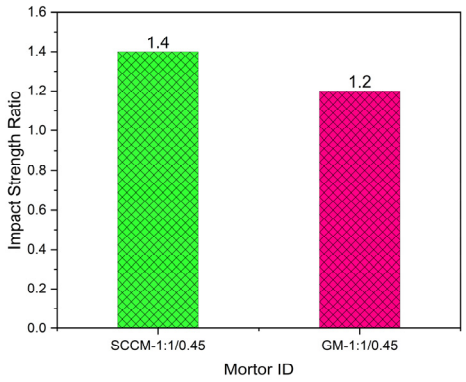

(b) Impact strength ratio

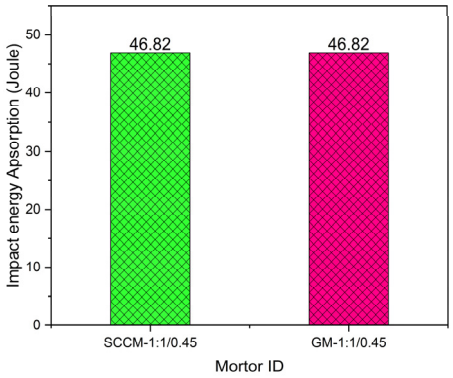

(c) Impact energy absorption

Fig. 13 Impact test results of mortars

Table 12 Rebound hammer test results of box beams

Grid No.	FBB – T40		GFBB – T40		GFBB – T50	
	Hammer Rebound [R]	Cube Compressive Strength (N/mm²)	Hammer Rebound [R]	Cube Compressive Strength (N/mm²)	Hammer Rebound [R]	Cube Compressive Strength (N/mm²)
1	36	37.50	36	37.50	37	39.00
2	37	39.00	36	37.50	36	37.50
3	36	37.50	37	39.00	37	39.00
4	36	37.50	36	37.50	37	39.00
5	37	39.00	36	37.50	36	37.50
6	36	37.50	37	39.00	37	39.00
7	36	37.50	37	39.00	36	37.50
8	36	37.50	36	37.50	37	39.00
Average		37.88		38.06		38.44

points, and Table 12 and Fig. 14 show the outcomes.

As shown in Table 12, the cube compressive strength of box beams that is calculated using hammer rebound is marginally lower than that discovered through compressive strength testing on geopolymer mortar cubes. According to IS 13311 (Part 2), NDT results might differ by up to 25% when comparing compressive strength. However, test results clearly demonstrate that all panels have the same strength (i.e., the uniformity).

3.2.2 Ultrasonic pulse velocity test results on box beams

Box beams were subjected to UPV testing in accordance with IS 13311-Part 1 (2004). Table 13 and Fig. 15 each display different grid lines that serve as markers for the panels. The transit time (T) and known path length (L) are used to calculate the pulse velocity (V = LxT).

3.2.3 Flexural strength of box beams

Table 14 provides the load and related deflection of box beams. Additionally, the stiffness, ductility, and amount of

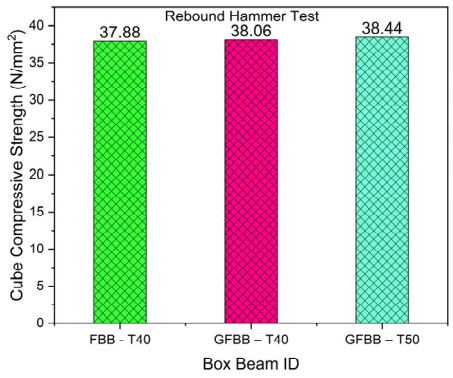

Fig. 14 Rebound hammer test results on ferro-cement and ferro-geopolymer box beams

Table 13 Ultrasonic pulse velocity test results of box beams

Grid No.	Pulse velocity (km/s)		
	FBB – T40	GFBB – T40	GFBB – T50
1	4.36	4.22	4.24
2	4.50	4.24	4.24
3	4.57	4.24	4.25
4	4.34	4.24	4.24
Average	4.44	4.235	4.243

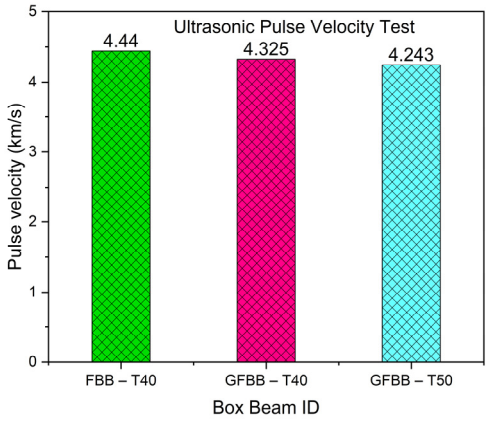

Fig. 15 Ultrasonic pulse velocity test results of ferro-cement and ferro-geopolymer box beams

absorbed energy are taken into account. Fig. 16 illustrate the calculated load-deflection variation for ferro-cement and ferro-geopolymer box beams. Figs. 17 and 18 display the

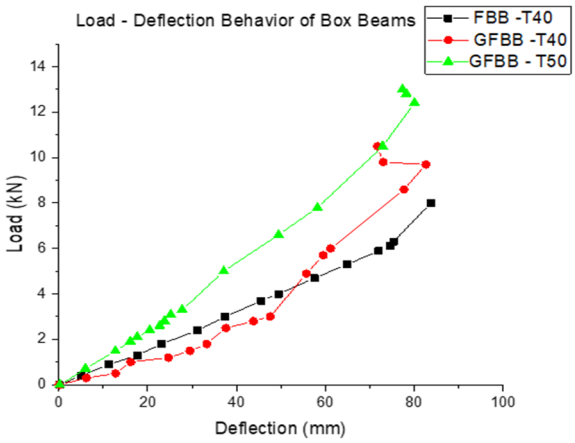

Fig. 16 Load - Deflection behavior of ferro-cement and ferro-geopolymer box beams

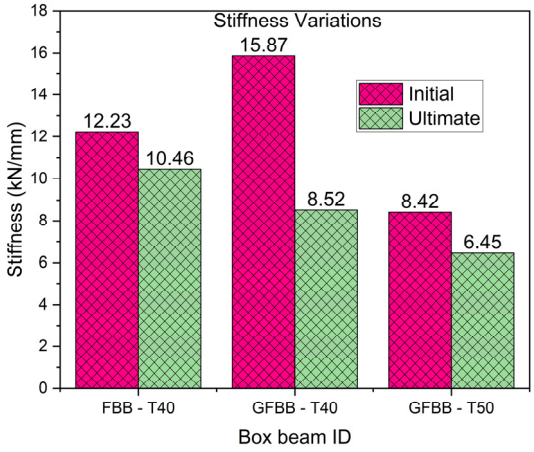

Fig. 17 Stiffness variation of ferro-cement and ferro-geopolymer box beams under flexure

stiffness, ductility index, and energy absorption in the final stage.

Ferro-cement and ferro-geopolymer box beams with 40 mm wall thicknesses have nearly equivalent load carrying capacities at the final stage. Furthermore, the ductility, and energy absorption have increased in the ferro-geopolymer box beam with a 40 mm wall thickness. It is also noticed that the initial stiffness increases which gradually decreases in ultimate stiffness by 18.55%. Additionally, the final deflection of ferro-geopolymer box beams with a 40 mm wall thickness is greater than 21.25%, despite the initial deflection being less than 36.17%.

Table 14 Box beams' load, deflection, and flexural strength

Box Beam ID	Cracking		Ultimate		Stiffness (kN/mm)		Ductility index	Energy absorption (Joule)
	Load (kN)	Deflection (mm)	Load (kN)	Deflection (mm)	Initial	Ultimate		
FBB-T40	57.50	4.70	83.70	8.00	12.23	10.46	1.70	379.89
GFBB- T40	47.60	3.00	82.60	9.70	15.87	8.52	3.20	494.44
GFBB- T50	27.80	3.30	80.00	12.40	8.42	6.45	3.76	535.6

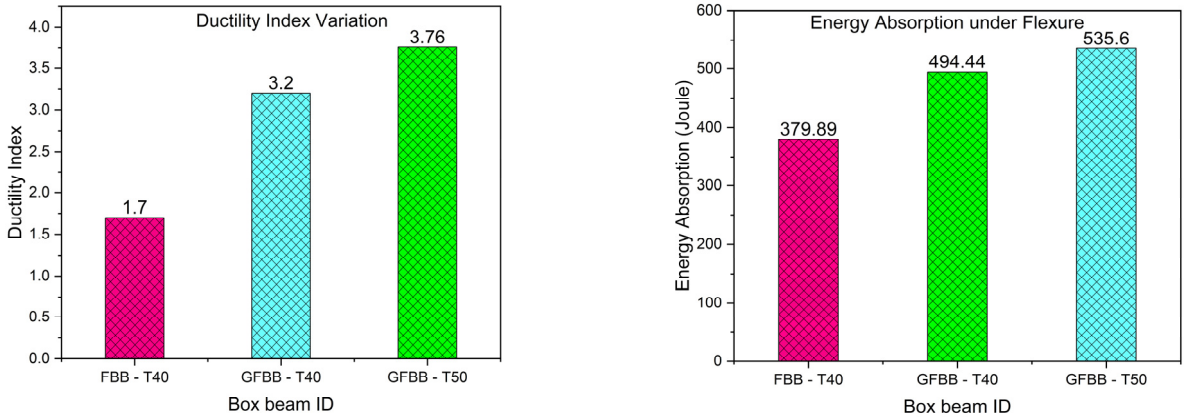

(a) Ductility variation (b) Energy absorption

Fig. 18 Ductility, and energy absorption of ferro-cement and ferro-geopolymer box beams

Fig. 19 Cracking characteristics of ferro-cement and ferro-geopolymer box beams under flexure

In comparison to ferro-geopolymer box beams with wall thicknesses of 40mm, the deflection, ductility, and energy absorption at the ultimate stage are increased by 27.84%, 17.50%, and 8.33% respectively as the wall thickness of the ferro-geopolymer box beams is increased to 50mm. However, the load carrying capacity and stiffness decrease by 3.15% and 24.30%, respectively. Every box beam exhibits the same shear failure mode.

3.2.4 Cracking behavior of box beams under flexure

Fig. 19 shows the ferro-cement and ferro-geopolymer box beams' cracking characteristics.

Preterm shear degradation was seen in every box beam as a result of the box beams' weak shear zone. However, as demonstrated in Fig. 19, by thickening the walls of the ferro-geopolymer beams, the order of failure/cracks was changed. As a result, there weren't more cracks in the beam before it broke, and the final phase of the failure was a desirable shear failure.

As a result of the test results, the following general conclusions have been drawn:

4. Conclusions

- The disposal of fly ash, a problem for the environment, is eliminated by the effective and extensive use of ASTM Class F - Indian fly ash in heat-cured geopolymer mortar. Fly ash, which was formerly thought of as waste, could be used in geopolymer cement and therefore can be used as a valuable commodity.
- The test findings demonstrate that fly ash-based geopolymer mortar has naturally self-compacting faces, hence no additional mix design technique is needed to prepare mortar.
- The ferro-geopolymer box beams are an environmentally benign structural component because they utilise fly ash which was considered a waste product since these aids in the entire replacement of cement, is also reduces greenhouse gas emissions. These two qualities of the geopolymer specimen lead to better solid waste management and more significant environmental pollution reduction.

- The ferro-geopolymer box beams' significant deflection indicates that they are more ductile than ferro-cement box beams and, therefore, provide adequate warning before failure.
- Ferro-cement and ferro-geopolymer box beams with walls that are 40 mm thick almost have equivalent load carrying capacities at the final stage. Additionally, the ferro-geopolymer box beam's initial stiffness, energy absorption, and ductility are all raised by 88.40%, 30.16%, and 29.77%, respectively, while the stiffness's final value is decreased by 18.55%. On the other hand, ferro-geopolymer box beams with a 40mm wall thickness exhibit a larger ultimate deflection of over 21.25%, and an initial deflection of less than 36.17%.
- When a ferro-geopolymer box beam's wall thickness is increased to 50 mm, the deflection, ductility, and energy absorption at the final stage are increased, by 27.84%, 17.50%, and 8.33%, respectively, when compared to ferro-geopolymer box beams with wall thickness 40 mm. However, the load carrying capacity and stiffness are decreased, respectively, by 3.15% and 24.30%.
- Preterm shear degradation was seen in all of the box beams as a result of the weak shear zone in the box beams. However, by thickening the walls of the ferro-geopolymer beams, the order of failure/cracks was changed. As a result, the beam only developed a few minor cracks before failing, and the last phase of the failure was a desirable shear failure.
- Heat curing, which replaces water-based curing, significantly reduces water consumption and product delivery time, resulting in cost. It also leads to a sustainable and efficient production.

Acknowledgments

The authors express their gratitude and thanks to the Management of Thiagarajar College of Engineering, Madurai and P.S.R. Engineering College, Sivakasi for facilitating this study. The authors are also thankful to the Management of Ramco Institute of Technology, Rajapalayam for their constant support towards research activities.

References

Abdulkadir, G., Metin, K. and Tolga, G.M. (2020), "An analysis of the usability of prefabricated cage-reinforced composite beams with self-compacting and lightweight concrete under flexural loads", *Constr. Build. Mater.*, **255**, 119274. https://doi.org/10.1016/j.conbuildmat.2020.119274

Abdullah, M.M.A., Hussin, K., Bnhussain, M., Ismail, K.N. and Ibrahim, W.M.W. (2011), "Mechanism and chemical reaction of fly ash geopolymer cement-a review", *Int. J. Pure Appl. Sci. Technol.*, **6**(1), 35-44.

ACI Committee 549 (1997), State-of-the-Art Report on Ferrocement, Report ACI 549-R97, American Concrete Institute, USA.

Ahmed, A. and Radhouane, M. (2015), "Structural performance of new fully and partially concrete-filled rectangular FRP-tube beams", *Constr. Build. Mater.*, **101**(1), 652-660. https://doi.org/10.1016/j.conbuildmat.2015.10.060

Aofei, G., Zhihui, S. and Jagannadh, S. (2021), "Experimental and finite element analysis on flexural behavior of mortar beams with chemically modified kenaf fibers", *Constr. Build. Mater.*, **292**(123449). https://doi.org/10.1016/j.conbuildmat.2021.123449

ASTM C494 (1999), Standard Specification for Chemical Admixtures for Concrete, ASTM Standards, USA.

ASTM C618-5 (2005), Standard Specification for Coal Fly Ash and Raw or Calcined Natural Pozzolan for Use in Concrete, ASTM Standards, USA.

ASTM D 2794-93 (2010), Standard test method for resistance of organic coatings to the effects of rapid Deformation (Impact), ASTM Standards, USA.

Bangladesh National Building Code-Part 6 (2012), Structural Design, Chapter12, Ferrocement Structures, **6**, 695-714.

BS EN 1015-3 (1999), Methods of test for mortar for masonry Determination of consistence of fresh mortar (by flow table), European Standards, CEN.

Construction Diagnostic Centre Pvt. Ltd. (CDC) (2020), Brochure 2020- For health assessment and risk evaluation of structures, Pune, India.

Davidovits, J. (1979), "Synthetic Mineral Polymer Compound of the Silicoaluminates Family and Preparation Process", US Patent No. 4472199.

Davidovits, J. (1994), "Global warming impact on the cement and aggregates industries", *World Resource Review*, **6**(2), 263-278.

EFNARC Guidelines (2002), Specification and Guidelines for Self-Compacting Concrete.

Francesco, D.M., Peter, C.R., Kees, B. and Michael, P. (2017), "Measuring resource efficiency and circular economy: A market value approach", *Resour. Conserv. Recycl.*, **75**(5)**,** 215-221. https://doi.org/10.1016/j.resconrec.2017.02.009

Glukhovsky, V.D. (1957), "Soil silicate-based products and structures", *Gosstroiizdat Publish. Kiev*, *USSR*.

Government of Maharashtra -Water Resources Department (2018), WRD Handbook Chapter no. 1 for Ferrocement Technology, Maharashtra Engineering Research Institute, Nashik, India.

Hardjito, D., Cheak, C.C. and Lee Ing, C.H. (2008), "Strength and Setting Times of Low Calcium Fly Ash-based Geopolymer Mortar", *Modern Appl. Sci.*, **2**(4), 3-11. https://doi:10.5539/mas.v2n4p3

Ibrahim, G.S., Yousry, B.S., Essam, L.E., Osama, A.K. and Peter, A.A. (2018), "Flexural characteristics of lightweight ferrocement beams with various types of core materials and mesh reinforcement", *Constr. Build. Mater.*, **171**, 802-816. https://doi.org/10.1016/j.conbuildmat.2018.03.167

International Energy Agency (IEA) (2022), CO_2 Emissions in 2022, France.

IS 13311 (Part 1) (2004), Non-Destructive Testing of Concrete - Methods of Test-Ultrasonic Pulse Velocity, Bureau of Indian Standards, New Delhi, India.

IS 13311 (Part 2) (2004), Non-Destructive Testing of Concrete - Methods of Test-Rebound Hammer, Bureau of Indian Standards, New Delhi, India.

IS 1489 (Part 1) (2005), Portland-Pozzolana cement Specification, Bureau of Indian Standards, New Delhi, India.

IS 1786 (2008), High Strength Deformed Steel bars and Wires for Concrete Reinforcement - Specification, Bureau of Indian Standards, New Delhi, India.

IS 3025 (Part 1) (1987), Methods of Sampling and Test (Physical and Chemical) for Water and Wastewater, Bureau of Indian Standards, New Delhi, India.

IS 3812 (Part 1) (2003), Pulverized Fuel Ash - Specification for use as Pozzolana in Cement, Cement Mortar and Concrete, Bureau of Indian Standards, New Delhi, India.

IS 383 (1997), Specification for Coarse and Fine Aggregates from Natural Sources for Concrete, Bureau of Indian Standards, New Delhi, India.

IS 4031 (Part 6) (1988), Methods of physical tests for hydraulic cement, Determination of compressive strength of hydraulic cement (other than masonry cement), Bureau of Indian Standards, New Delhi, India.

IS 5816 (1999), Methods of Tests for Split Tensile Strength of Concrete Cylinders, Bureau of Indian Standards, New Delhi.

IS 9103 (2004), Concrete Admixtures – Specification, Bureau of Indian Standards, New Delhi, India.

Kuhl, H. (1908), "Slag Cement and Process of Making the Same", 900,939.

Nabila, S., Mohamed, O.A., Enas, T.S., Mohammad, A.A. and Olabid, A.G. (2022), "Geopolymer concrete as green building materials: Recent applications, sustainable development and circular economy potentials", *Sci. Total Environ*., **836**, 155577. https://doi.org/10.1016/j.scitotenv.2022.155577

Naghizadeh, A. and Ekolu, S.O. (2019), "Method for comprehensive mix design of fly ash geopolymer mortars", *Constr. Build. Mater*., **202**, 704-717. https://doi.org/10.1016/j.conbuildmat.2018.12.185

Okamura, H. and Ouchi, M. (2003), "Self compacting concrete", *J. Adv. Concrete Technol*., **1**(1), 5-15. http://dx.doi.org/10.3151/jact.1.5

Ouellet-Plamondon, C. and Habert, G. (2015), "Life cycle assessment (LCA) of alkali-activated cements and concretes", *Handbook of Alkali-Activated Cements*, *Mortars and Concretes*, 663-686. https://doi.org/10.1533/9781782422884.5.663

Palomo, A., Krivenko, P., Garcia-Lodeiro, I., Kavalerova, E., Maltseva, O. and Fernández-Jiménez, A. (2014), "A review on alkaline activation: new analytical perspectives", *Mater. Construcc*., **64**, 315. http://dx.doi.org/10.3989/mc.2014.00314

Palomo, A., Maltseva, O., Garcia-Lodeiro, I. and Fernández-Jiménez, A. (2021), "Portland Versus Alkaline Cement: Continuity or Clean Break: A Key Decision for Global Sustainability", *Frontiers in Chemistry*, **9**, 705475. https://doi.org/10.3389/fchem.2021.705475

Parthiban, N. and Neelamegam, M. (2017), "Flexural behavior of reinforced concrete beam with hollow core in shear section", *Int. Res. J. Eng. Technol*. (*IRJET*), **4**(4). https://www.irjet.net/archives/V4/i4/IRJET-V4I4573.pdf

Pierrehumbert, R. (2019), "There is no Plan B for dealing with the climate crisis", *Bull. Atomic Scient*., **75**(5), 215-221. https://doi.org/10.1080/00963402.2019.1654255

Peng, Z., Kexun, W., Juan, W., Jinjun, G., Shaowei, H. and Yifeng, L. (2020), "Mechanical properties and prediction of fracture parameters of geopolymer/alkali-activated mortar modified with PVA fiber and nano-SiO_2", *Ceram. Int*., **46**(12), 20027-20037. https://doi.org/10.1016/j.ceramint.2020.05.074

Perry, R.H. (1997), Perry's Handbook for Chemical Engineers, McGraw – Hill, USA.

Portland Cement Association (PCA) Report (2019), Washington.

Provis, J.L. (2014), "Geopolymers and other alkali activated materials: why, how, and what?", *Mater. Struct*., **47**, 11-25. https://doi.org/10.1617/s11527-013-0211-5

Provis, J.L. and Van Deventer, J.S.L. (2009), "Geopolymers-Structure, processing, properties and industrial applications", Woodhead publishing limited, Cambridge, UK. www.woodheadpublishing.com

Purdon, A. (1940), "The action of alkalis on blast-furnace slag", *J. Soc. Chem. Ind*., **59**, 191-202.

Robbie, M.A. (2018), "Global CO_2 emissions from cement production", *Earth Syst. Sci. Data*, **10**, 195-217. https://doi.org/10.5194/essd-10-195-2018

Sakkarai, D. and Soundarapandian, N. (2021), "Strength behavior of flat and folded fly ash-based geopolymer ferrocement panels under flexure and impact", *Adv. Civil Eng*., **2021**(2311518). https://doi.org/10.1155/2021/2311518

Shannag, M.J. and Mourad, S.M. (2012), "Flowable high strength cementitious matrices for ferrocement applications", *Constr. Build. Mater*., **36**, 933-939. https://doi.org/10.1016/j.conbuildmat.2012.06.051

Temuujin, J., Riessen, A.V. and Mackenzie, K.J.D. (2010), "Preparation and characterisation of fly ash based geopolymer mortars", *Constr. Build. Mater*., **24**, 1906-1910. https://doi.org/10.1016/j.conbuildmat.2010.04.012

Tran, D.H., Kroisova, D., Louda, P., Bortnovsky, O. and Bezucha, P. (2009), "Effect of curing temperature on flexural properties of silica-based geopolymer-carbon reinforced composite", *J. Achieve. Mater. Manuf. Eng*., **37**(2), 492-497. http://jamme.acmsse.h2.pl/papers_vol37_2/37238.pdf

Xie, J. and Kayali, O. (2016), "Effect of superplasticiser on workability enhancement of Class F and Class C fly ash-based geopolymers", *Constr. Build. Mater*., **122**, 36-42. https://doi.org/10.1016/j.conbuildmat.2016.06.067

JKK